Journal of Sound and Vibration 329 (2010) 3397–3416

Contents lists available at ScienceDirect

Journal of Sound and Vibration

journal homepage: www.elsevier.com/locate/jsvi

Reproduction and application of human bouncing and jumping forces from visual marker data

V. Racic *, J.M.W. Brownjohn [1], A. Pavic [2]

Department of Civil and Structural Engineering, University of Sheffield, Sir Frederick Mappin Building, Sheffield S1 3JD, UK

ARTICLE INFO

Article history:
Received 22 September 2009
Received in revised form
22 February 2010
Accepted 23 February 2010
Handling Editor: H. Ouyang
Available online 21 March 2010

ABSTRACT

State-of-the-art facilities for measuring bouncing and jumping ground reaction forces (GRFs) comprise typically equipment for direct force measurement, i.e. single or multiple floor-mounted force plates. Artificial laboratory conditions and constraints imposed by the direct measurement systems, such as the small measuring area of a force plate, can have a strong influence on human ability to bounce and jump, naturally yielding unrepresentative force data. However, when dealing with issues like vibration serviceability assessment of real full-scale structures, such as floors, footbridges, staircases and grandstands, there is a growing need to estimate realistic GRFs under a wide range of natural conditions. This paper presents a novel method in the civil engineering context utilising 'free-field' measurement of human bouncing and jumping forces recorded continuously in time using motion capture technology transferred and adapted from biomechanical research. Results show that this kind of data can be used successfully in studies of human–structure dynamic interaction, specifically negative cue effect of a perceptibly vibrating structure on GRFs, energy flow and power in the human–structure system, and also synchronisation between individuals when bouncing/jumping in groups on more or less perceptibly moving structures.

1. Introduction

In the last 10 years, there have been increasing numbers of grandstands [1,2] and entertainment venues [3] that have failed to perform satisfactorily when occupied and dynamically excited by multiple persons and large crowds bouncing and/or jumping in unison. These mostly vibration serviceability problems have indicated high levels of uncertainty with which civil structural engineers are faced nowadays when designing any of the above mentioned structures which require vibration performance assessment.

There have been numerous attempts to provide reliable and practical descriptions of human bouncing and jumping loads by measuring the contact forces between the ground and test subjects, hence generally known as ground reaction forces (GRFs). For this purpose Ebrahimpour et al. [4] and Pernica [5] designed a 'force platform', whereas Rainer et al. [6] used the continuously measured reaction of a floor strip having known dynamic properties. Much research into GRFs has been done in the biomechanics community, as GRF pattern analyses provide useful diagnostics in medical and sports applications [7,8]. Therefore, it is not surprising that the present state-of-the-art equipment for these force measurements,

* Corresponding author. Tel.: +44 114 222 5727; fax: +44 114 222 5700.
E-mail addresses: v.racic@sheffield.ac.uk (V. Racic), james.brownjohn@sheffield.ac.uk (J.M.W. Brownjohn), a.pavic@sheffield.ac.uk (A. Pavic).
[1] Tel.: +44 114 222 5771.
[2] Tel.: +44 114 222 5721.

0022-460X/$ - see front matter © 2010 Elsevier Ltd. All rights reserved.
doi:10.1016/j.jsv.2010.02.021

i.e. the 'force plate', emerged from the field of biomechanics of human gait. However, there are a few disadvantages of force plates that make them less suitable in vibration serviceability assessment of civil engineering structures.

Firstly, standard dimensions of force plates (typically $0.6 \times 0.4\,\mathrm{m}$) are not large enough to accommodate jumping for some individuals who must control and target their jumps to the relatively small force plate area so as to allow adequate recordings. As a result, this targeting effort can affect ability to jump naturally and therefore alter GRF patterns [8].

Secondly, force plates cannot provide accurate measurements when mounted on a flexible structure due to their self-inertia. This is because they behave like accelerometers and produce outputs including inertia forces of the moving support surface [9]. Therefore a typical experimental setup includes force plates mounted on a rigid laboratory floor, thus limiting the measurements to laboratory conditions. However, when investigating issues related to vibration serviceability there is a growing need for monitoring many subjects during daily life activities in a natural environment, such as office, sport facility, or a footbridge.

Bearing all these in mind, one way forward is an alternative experimental approach to avoid all the drawbacks of force plates. Several biomechanical studies designed to estimate the contribution of motion of various body segments to vertical GRFs [10–12] offer a step in this direction. Using these biomechanical studies as a solid foundation, this paper aims to present a reader, conversant with vibration serviceability problems of civil engineering structures, with a novel method, in the context of a civil engineering application, utilising 'free-field' measurement to obtain bouncing and jumping GRFs in a wide range of conditions. The free-field measurement applies the method to estimate the forces in the real world (i.e. naturally occurring environments) rather than in a constrained laboratory setting. The method will also enable study of areas of significant interest and lacking in knowledge, specifically human–structure dynamic interaction and coordination of movements between a number of people bouncing/jumping on more or less perceptibly moving structures.

In the context of this paper, human–structure dynamic interaction aims to address two related key issues. Firstly, how perceptible structural vibrations can influence forces induced by active human occupants, and secondly, how active human occupants influence the dynamic properties (modal mass, damping and stiffness) of a civil engineering structure they occupy and dynamically excite.

2. Theoretical background

According to Newton [13], the origin of dynamic forces is in momentum changes, which, for constant mass, derives from the product of mass and acceleration. As applied to the human body, the vertical force acting upon the body (i.e. vertical ground reaction force F_{GR}) is equal to the product of the body mass m, concentrated at a single point referred to as the body centre of mass (CoM), and its acceleration [12]:

$$F_{GR} = ma_{CoM} - mg = m(a_{CoM} - g) \tag{1}$$

In this equation g is the static acceleration due to gravity and a_{CoM} is the dynamic acceleration due to body motion (noting that upward accelerations are defined as positive, hence $g = -9.81\,\mathrm{m/s^2}$ in the UK). The body CoM represents the centroid of the total mass of the multi-segment human body system.

Taking more accurate mass distribution into account and assuming that the body is subdivided into s rigid segments, such as head, arms, thorax and legs, Eq. (1) becomes [12]

$$F_{GR} = \sum_{i=1}^{s} m_i(a_i - g) \tag{2}$$

where m_i and a_i are mass and acceleration of the centre of the mass of the i-th body segment, respectively. This relation implies that the force a person generates against the surface must react against inertia of their body, so that the sum of products of masses and accelerations for all body parts must equal the GRF at all times. Similar to earthquake engineering, excitation is due to inertia forces, which generate internally balanced forces through the human body. The summation of all these forces is transmitted ultimately to the support of the body and results in the GRF. This is the key principle behind the idea of estimating GRFs via measuring motion of body segments.

Although each body segment represents the portion of the human body composed of a bony part and soft tissue, the human body is commonly modelled as a kinematic chain of rigid body segments hypothetically joined with spherical hinges [10–12]. Not all body joints are in fact spherical hinges, but for the purposes of this analysis, there is no loss of generality in this assumption. To estimate physical parameters associated with each rigid segment, such as mass and position of its centre, several biomechanical methods have been proposed so far. Regression equations generated from cadaver data [14,15] and data from live humans [16,17] have been the most popular analytical approach, mainly because they can provide estimates of these parameters quickly and easily.

In this study measurement of body motion used optical motion capture technology rather than inertial sensors (accelerometers) due to practical difficulties. Wires and cables place restrictions on the ability to measure patterns of human locomotion without unwanted artefacts that could mask the natural patterns of motion. On the other hand, applications of wireless technology for accurately measuring 3D human body kinematics have been limited by the lack of reliable and affordable technology to provide synchronised data recordings in a common axis system from multiple inertial sensors.

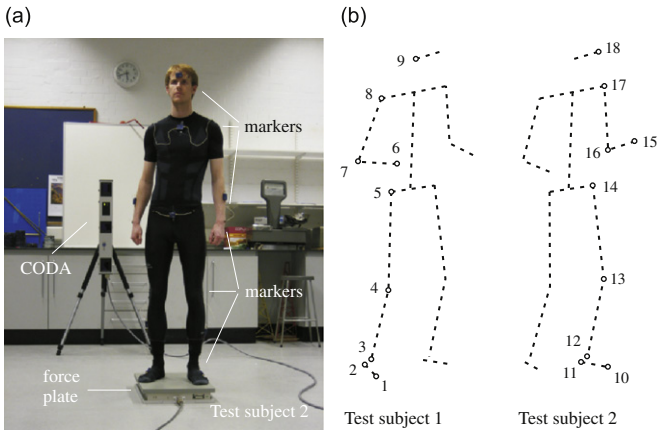

Fig. 1. (a) Experimental setup. (b) Human body model and arrangement of markers.

Most modern motion capturing systems use video-based optoelectronic technology, such as cameras or sensors, to quantify position and orientation of bodies in real time [18]. If a device is optoelectronic, it means that it interacts with light. The three-dimensional (3D) representation of body movement is reconstructed from optical sources attached to the skin's surface and serve as target markers (Fig. 1a and b). The markers are placed in a manner to satisfy technical requirements such as high visibility from sensors and to minimise relative displacement between them and underlying bone during movement [18]. The latter is important since the assumption of rigid body segments has been made. However, the choice of where and how to place target markers to minimise error in measurements is a significant issue on its own [18]. More detailed explanation of this issue can be found in a comprehensive literature review article published recently by the authors [19].

The strategy for verifying the method described by Eq. (2) is as follows:

(1) Measure directly the vertical jumping/bouncing force using a floor-mounted three-axial force plate and synchronously record the motion of target markers attached to different body segments using optoelectronic technology. Compare the reproduced forces with their directly measured counterparts.
(2) Employ the same test subjects in a separate but nominally identical test and measure simultaneously motion of their bodies and vertical response of a simple structure whose modal properties (of the empty structure) have previously been obtained from modal testing.
(3) Perform forward response analysis by utilising the reproduced human induced loading in conjunction with the known modal properties of vertical modes of the empty test structure.
(4) Compare these responses with their measured counterparts.

To determine the modal properties of the empty unoccupied test structure, experimental modal testing was preferred over analytical finite element modelling. There are two reasons for this decision: firstly, modal testing is a more accurate method, and secondly, the study presented in this paper was designed to use a full experimental approach wherever possible. The next section goes into details of data collection.

3. Experimental investigation

All preparatory steps necessary for the launch of the experiments are explained in Section 3.1. The experiments alone comprise three types of measurements, i.e.

(1) synchronous acquisition of direct force measurement and body motion data due to jumping/bouncing on a rigid laboratory floor (Section 3.2),
(2) modal testing of a simple test structure (Section 3.3) and
(3) synchronous monitoring of body motion and structural response due to jumping/bouncing on the structure, performed in a manner nominally identical to that used in the direct force measurement (Section 3.4).

3.1. Preparatory phase

Two male volunteers (age 27 and 30 years, body mass 70 and 67 kg) participated in the experiment. The test protocol, approved by the Research Ethics Committee of the University of Sheffield, required that the participants complete a physical activity readiness questionnaire and a preliminary fitness test (measuring blood pressure and resting heart rate) to check whether they were suited to the kind of physical activity required during the experiments. The test subjects were

non-restrictive sportswear, as shown in Fig. 1a. Prior to testing, the test subjects received a 10 min warm-up supervised by a qualified instructor, comprising stretching, bouncing and jumping at self-selected rates.

Using a modelling strategy proposed by de Leva [17], 15 body segments and corresponding segmental masses and positions of segmental mass centres of each participant were defined. The segmentation comprised the pairs of the feet, the shanks, the thighs, the hands, the forearms, the upper-arms, as well as the pelvis, the trunk, and the head. The segmental ends were defined via nine target markers stuck to the head and major body joints such as ankle, wrist, knee or elbow, as illustrated in Fig. 1b. Because the number of available markers is limited, as well as to reduce the subject's preparatory time and to enable simple and time-efficient experiments, symmetry of motion in the vertical plane between the left and right body segments was assumed.

3.2. Direct force measurements coupled with body motion data

The best way to validate the procedure for recovering GRFs from body motion data is to compare the forces calculated using Eq. (2) with those measured simultaneously and directly by a force plate attached to a rigid surface. All bouncing and jumping forces were recorded by an AMTI BP-400600 force plate [9] rigidly fixed to the laboratory floor (Fig. 1a). Vertical movement of tracking markers was monitored continuously in time using Codamotion technology [20]. A Codamotion host computer (Active Hub) enabled simultaneous data acquisition from multiple sets of Codamotion sensors (in this case two) and the AMTI force plate. This allowed synchronous acquisition of the analogue outputs from the force plate and Coda sensors, so both forces and the body motion data were sampled at 200 Hz.

Each test subject was asked to jump to a given constant metronome beat at eight different jumping and bouncing frequencies in the range 1.4–2.8 Hz with increments of 0.2 Hz. The range included slow and fast rates commonly cited in the literature as comfortable for individuals [21]. Jumping and bouncing experiments were performed with frequencies in a quasi-random order and lasted for 25 s with 2 min rest between each, which both participants considered sufficient. The subjects were not given any explicit instructions about their jumping technique, but they were encouraged to move as if they were enjoying a lively concert or an aerobic exercise.

Examples of the force plate records and Codamotion data are given in Figs. 2 and 3, respectively.

3.3. Test structure and experimental modal analysis

The test structure is a 15 ton pre-stressed concrete slab strip situated in the Light Structure Laboratory at the University of Sheffield, UK. The slab strip is 11 m long and 2 m wide and structurally it presents a simply supported beam (Figs. 4 and 8).

The natural frequencies, modal masses, modal damping ratios and mode shapes of the structure were determined by shaker modal testing, as described in Section 3.3.1. Because the structure is quite flexible and can experience significant and visible deflections due to jumping/bouncing, this was followed by a simple system identification exercise, described in Section 3.3.2 to ascertain its modal properties and their amplitude dependence.

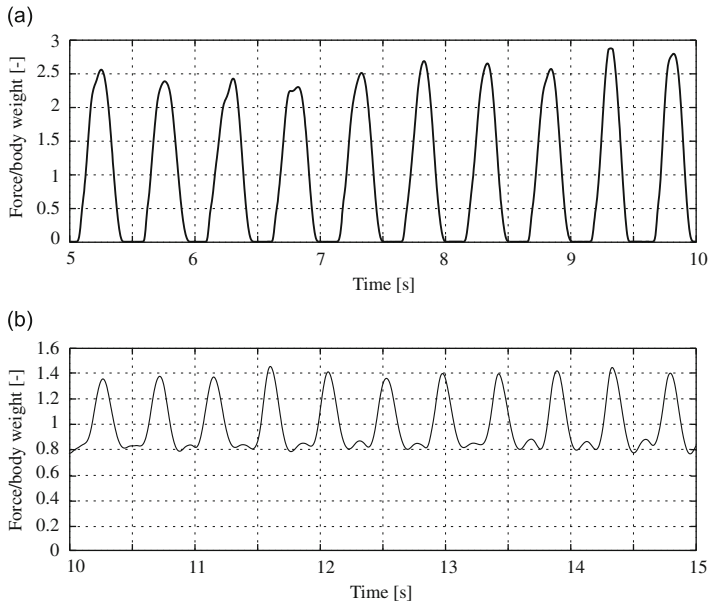

Fig. 2. Examples of directly measured forces due to TS 1: (a) jumping and (b) bouncing in response to constant metronome beats at 2 Hz.

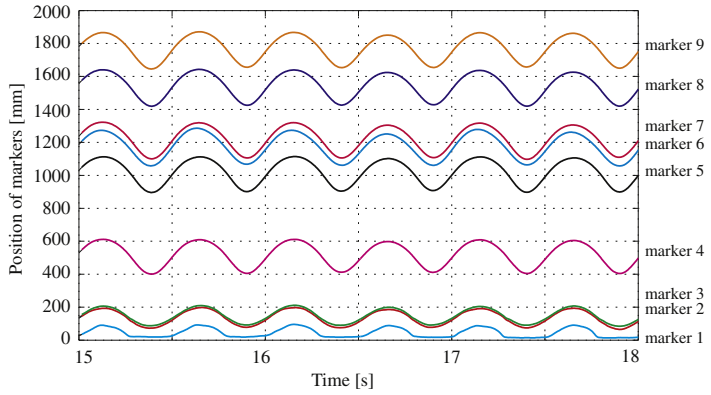

Fig. 3. Examples of marker vertical position (relative to the reaction surface) time histories due to TS 1 jumping in response to regular metronome beats at 2 Hz.

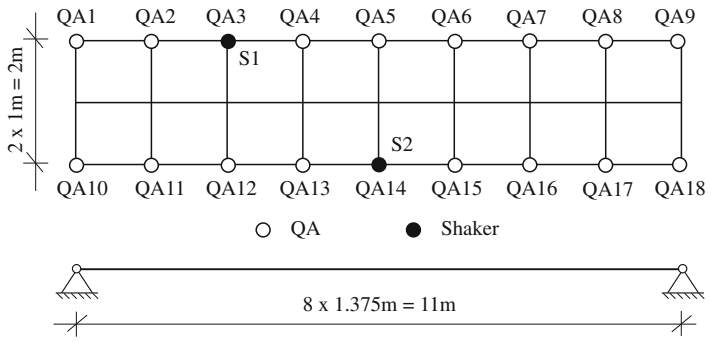

Fig. 4. Test grid for slab strip.

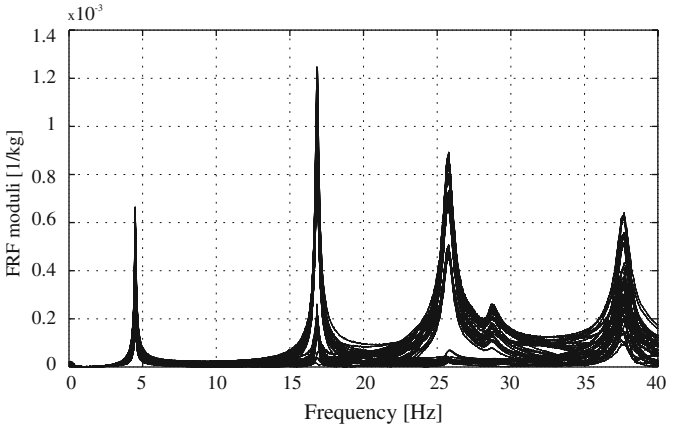

Fig. 5. FRF moduli between shaker excitations at S1 and S2 and the accelerations measured by 18 accelerometers arranged according to Fig. 4.

3.3.1. *Shaker testing*

Modal testing of the slab strip was performed using two APS-113 electro-dynamic shakers [22] positioned in the centre and a quarter span of the structure (Fig. 4). Vertical vibration response due to the random vertical shaker excitation was monitored using 18 QA750 accelerometers [23], positioned as illustrated in Fig. 4.

Using the synchronously measured shaker excitations and structural responses, the corresponding frequency response functions (FRFs) were calculated and moduli of these are shown in Fig. 5. In addition, the modal properties are reported in Fig. 6.

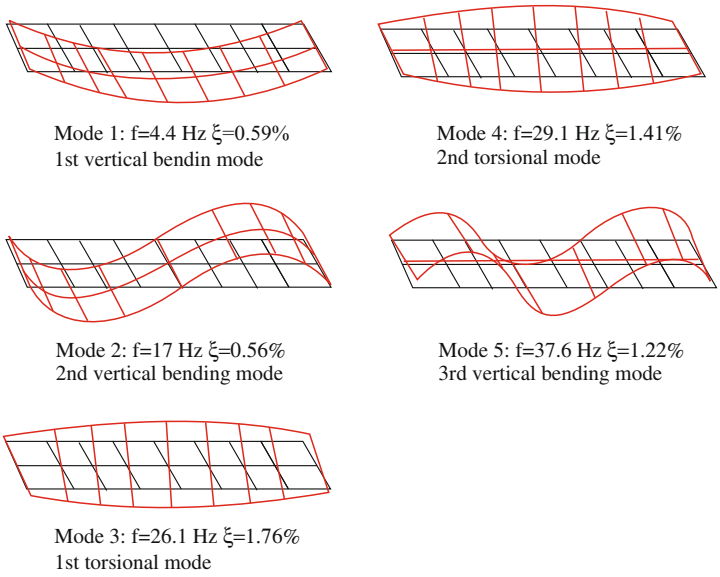

Fig. 6. Experimentally estimated modal properties on the test structure (first three vertical bending modes, first two torsional modes).

The results presented in Figs. 5 and 6 indicate that if either jumping or bouncing is performed in the middle of the span, the structure will predominantly respond in the first vertical mode. This is because most of the excitation energy is concentrated below 25 Hz and the second vertical mode is likely to have a node close to where the force is applied.

There are two similar looking torsion modes with distinctive natural frequencies due to slightly different support conditions on the strip ends.

3.3.2. *Nonlinearity of test structure*

The test structure is very slender and can vibrate in a wide amplitude range, from levels barely perceptible to occupants to visibly large amplitudes depending on the level and frequency of the excitation. Therefore, it was reasonable to check if the structure has amplitude dependent nonlinear characteristics, i.e. that the modal properties depend on the response level.

To test the hypothesis of nonlinearity, the structure was excited close to resonance by a well trained test subject jumping at 2.2 Hz in the middle of the span. The near-resonant response was caused by the second dominant harmonic of the induced jumping force at approximately 4.4 Hz. When the large acceleration levels were achieved (approximately 6 m/s^2), the test subject was asked to jump off the structure and accelerations at mid-span were recorded during the free vibration decay. There were two reasons for not using the shakers in this test. Firstly, even both shakers acting together were not powerful enough to induce vibration amplitudes comparable to those due to jumping. Secondly, the shakers would still generate some dynamic force during the free decay, even when disconnected or deactivated, and their mass contributes to the mass of the structure.

The amplitude (acceleration) dependent damping ratio and natural frequency of the first vertical mode were computed from the free decay using *MODAL* software [24]. It was clear that the vertical response of the structure was dominated by the first vertical mode so that the structure can be modelled as a single degree of freedom (SDOF) system by ignoring the effect of other modes. Fig. 7 shows cycle-by-cycle fitted fundamental frequencies and damping ratios.

Eqs. (3) and (4) curve fit the nonlinear damping ratio ξ (Fig. 7a) and frequency f (Fig. 7b), respectively:

$$\xi = \xi(a) = 0.831e^{-0.027a} - 0.507e^{-1.061a} \text{ (percent)} \tag{3}$$

$$f = f(a) = \frac{4.296a^3 + 12.30a^2 + 3.342a + 0.274}{a^3 + 2.758a^2 + 0.748a + 0.061} \text{ (Hz)} \tag{4}$$

Here $a = a(t)$ is the time dependent amplitude of the acceleration of the structure given in m/s^2. Using Eqs. (3) and (4), the nonlinear stiffness and damping coefficient can be expressed as

$$k = k(a) = m(2\pi f(a))^2 \text{ (N/m)} \tag{5}$$

$$c = c(a) = 2\xi\sqrt{km} \text{ (Ns/m)} \tag{6}$$

where $m = 6500$ kg is the modal mass which is assumed to be constant. These parameters are used in Section 4.2 to simulate the structural response under human-induced loads.

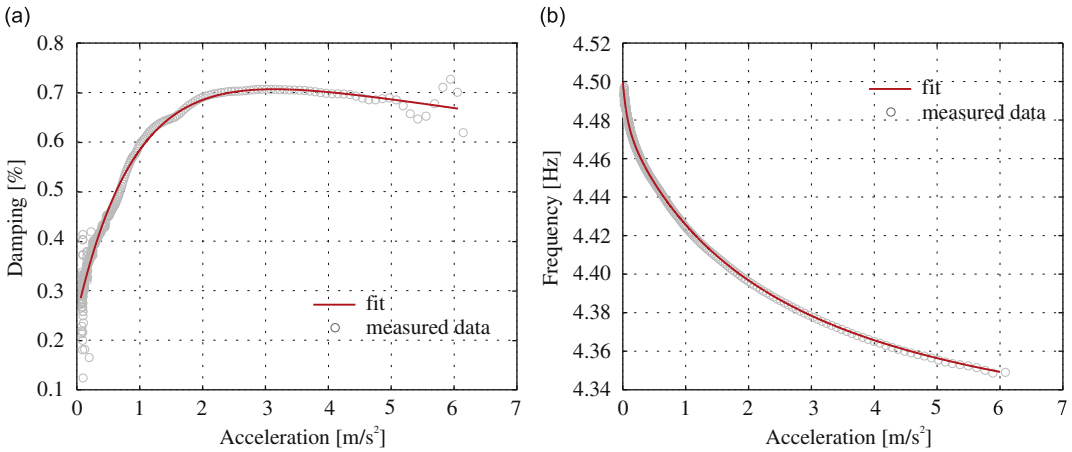

Fig. 7. Experimentally estimated nonlinear (a) damping and (b) fundamental frequency as functions of acceleration response level up to 6 m/s^2 at the mid-span.

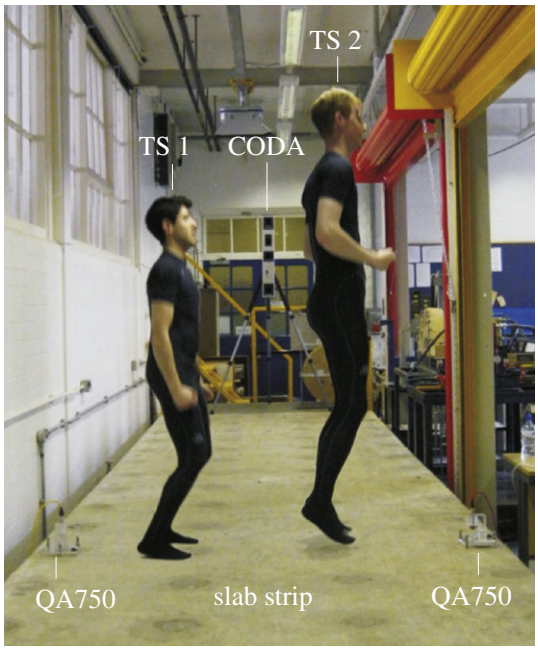

Fig. 8. Two test subjects jumping together on the slab strip.

3.4. *Body motion data coupled with response measurements of structure*

Each test subject, fully instrumented with the Coda markers, was asked to either jump or bounce alone in the mid-span of the structure in response to regular metronome beats at three different tempos: 2, 2.2 and 2.5 Hz. Note that jumping and bouncing at 2.2 Hz excited the structure as near to resonance as possible by the second harmonic of the corresponding forces. On the other hand, closely spaced tempos at 2 and 2.5 Hz excited the structure at frequencies out of resonance. Nominally identical tests were repeated when the two test subjects were jumping/bouncing together (Fig. 8).

The Codamotion host computer enabled simultaneous acquisition of vertical movement of the body markers and of the response of the structure measured in the middle of the span by both a QA750 accelerometer and a tracking marker. Both body motion data and vibration response were sampled at 200 Hz.

The aim was to calculate the response of the structure by using the forces reproduced from the body motion data and the modal properties of the first vertical mode determined in Section 3.3. A good match between the calculated and directly measured accelerations should provide a proof that the forces can be reproduced successfully. This is the key aspect outlined in the next section, together with the possibility to use the reproduced forces in a study of human–structure dynamic interaction and synchronisation of people when jumping/bouncing in groups.

4. Indirectly measured human-induced forces

Movement of the skin relative to the underlying bone is one of the major sources of error when reconstructing human-induced forces from body motion data [19]. This is known as 'soft tissue artefact' and is dominant during highly accelerated movements, e.g. when the feet abruptly hit the ground. Skin markers then oscillate considerably in an unsteady way with respect to the underlying bone, inducing high-frequency noise in the marker position (displacement) data. To filter out the noise, a fourth-order low-pass digital Butterworth filter (LPF) having cut-off frequency at 15 Hz was applied to displacements of all markers [19]. These displacements were then differentiated twice with respect to time to obtain accelerations of each tracking marker. Fig. 9 illustrates accelerations of the hip marker obtained with and without filtering out the noise above 15 Hz from the displacement data. It can be seen that the main visible features of the markers' accelerations representing the whole body segment motion remain intact after filtering.

In the next two sections, filtered acceleration time histories of the kind given in Fig. 9 are used in conjunction with information about the values and locations of the segmental masses (see Section 3.1) to calculate the GRF time histories according to Eq. (2). The method is first verified in Section 4.1 based on the comparison between directly measured and calculated (reproduced) forces on the stiff laboratory floor. This is followed in Section 4.2 by analysis of the reproduced forces induced on the moving test structure.

4.1. Model verification

The procedure for recovering GRFs from the body kinematics was validated using the data collected in Section 3.2. Vertical accelerations of the centres of mass of the 15 body segments were derived from the vertical accelerations of the nine target markers (Fig. 1b). The forces were calculated using Eq. (2) and then compared with those measured

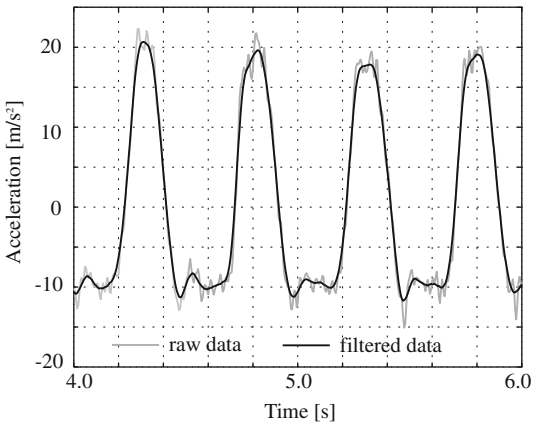

Fig. 9. Raw and filtered accelerations (LPF=15 Hz) of a hip marker due to jumping at 2 Hz.

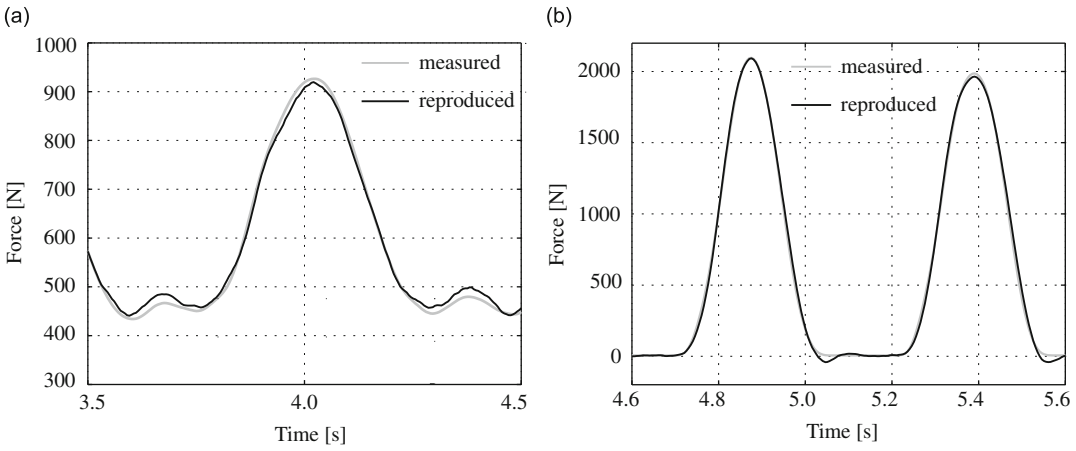

Fig. 10. Examples of reproduced (a) bouncing and (b) jumping forces due to a single person jumping at 2 Hz.

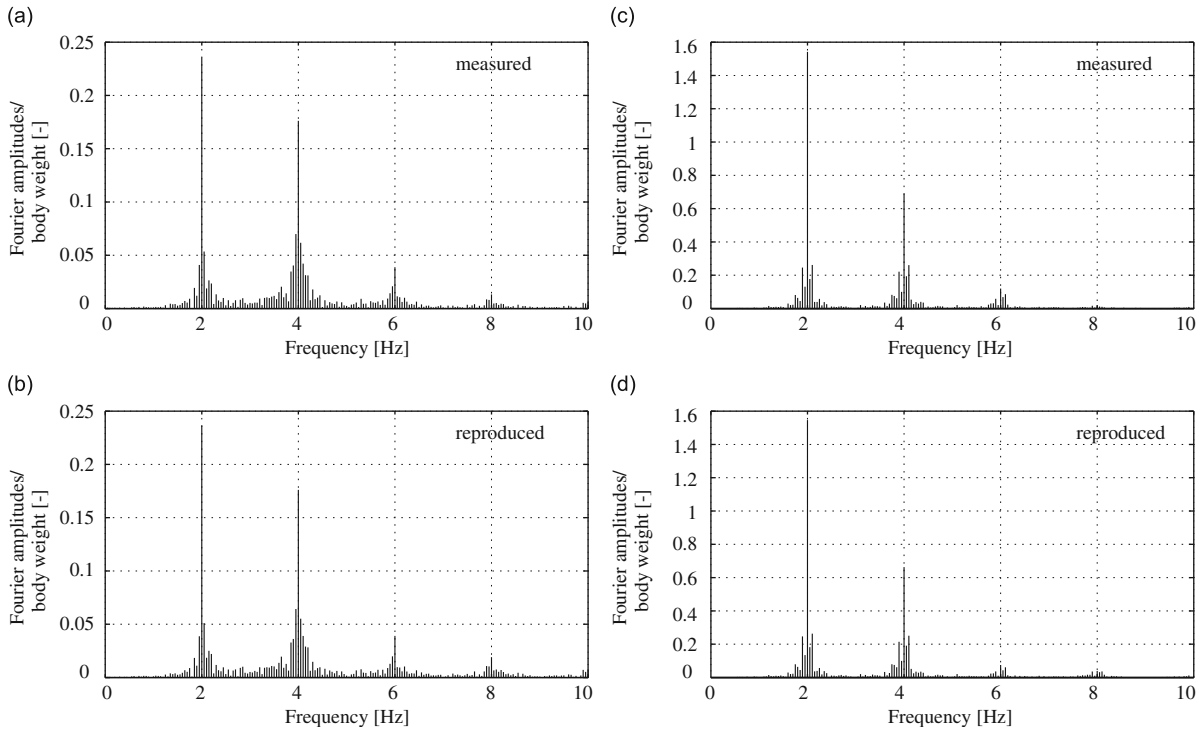

Fig. 11. Comparison between directly measured and reproduced (a, b) bouncing and (c, d) jumping forces in the frequency domain. Each Fourier amplitude spectrum was derived from a single 20-s long force signal (Fig. 10) without the use of averaging.

simultaneously and directly by the force plate. Fig. 10 illustrates examples of the comparison between measured and reproduced forces in time domain. Also, the corresponding frequency spectra are compared in Fig. 11.

Broadly speaking for all jumping and bouncing tests, the first dominant harmonic was reproduced with a difference $< \pm 2$ percent, the second dominant harmonic with a difference within the range of ± 4 percent, whereas for the third dominant harmonic the difference between directly measured and calculated forces was in the range of ± 7 percent. Moreover, relative error in the area under the graph of the spectra below 15 Hz was < 5 percent. All these indicated good matching in the frequency content between the measured and reproduced GRF signals.

4.2. Forces induced on test structure

The study presented in the next two sections is based on the experimental data collected as explained in Section 3.4. Section 4.2.1 presents analysis of the reproduced GRFs which test subjects generated when either bouncing or jumping alone on the test structure. This is followed by analysis of the group forces in Section 4.2.2.

4.2.1. Single test subject

Using the concept presented in the previous section, the force time histories generated in the mid-span of the structure when test subjects were bouncing or jumping alone in response to the regular metronome beats (at 2, 2.2 and 2.5 Hz) were reproduced from body motion data collected in Section 3.4. As an illustration, the reproduced force signals for test subject (TS) 1 are given in Fig. 12. The corresponding Fourier amplitude spectra in the vicinity of the second dominant harmonic are given in Fig. 13.

Since the forces have not been measured directly and synchronously with the body motion data (as was the case with the stiff surface), the next best way to check if the reproduced forces are correct is to compare responses of the structure measured directly by the accelerometers (Section 3.4) and those calculated from the corresponding SDOF model of the structure. The latter can be obtained using the reproduced forces as the forcing function together with the nonlinear modal properties of the first vertical mode measured in Section 3.3.

A good match between the calculated and directly measured accelerations in the mid-span of the structure (Fig. 14) strongly suggests that the forces have been reproduced successfully. Strong Fourier amplitudes at 4 and 5 Hz and slight 'spread' of energy to adjacent spectral lines in Fig. 13 indicate that TS 1 could follow metronome beats well when jumping and bouncing at 2 and 2.5 Hz, respectively. However, for jumping and bouncing at 2.2 Hz, the spread of energy is more prominent around 4.4 Hz. The same effect was observed for TS 2 as well. This indicated that it was more difficult for them

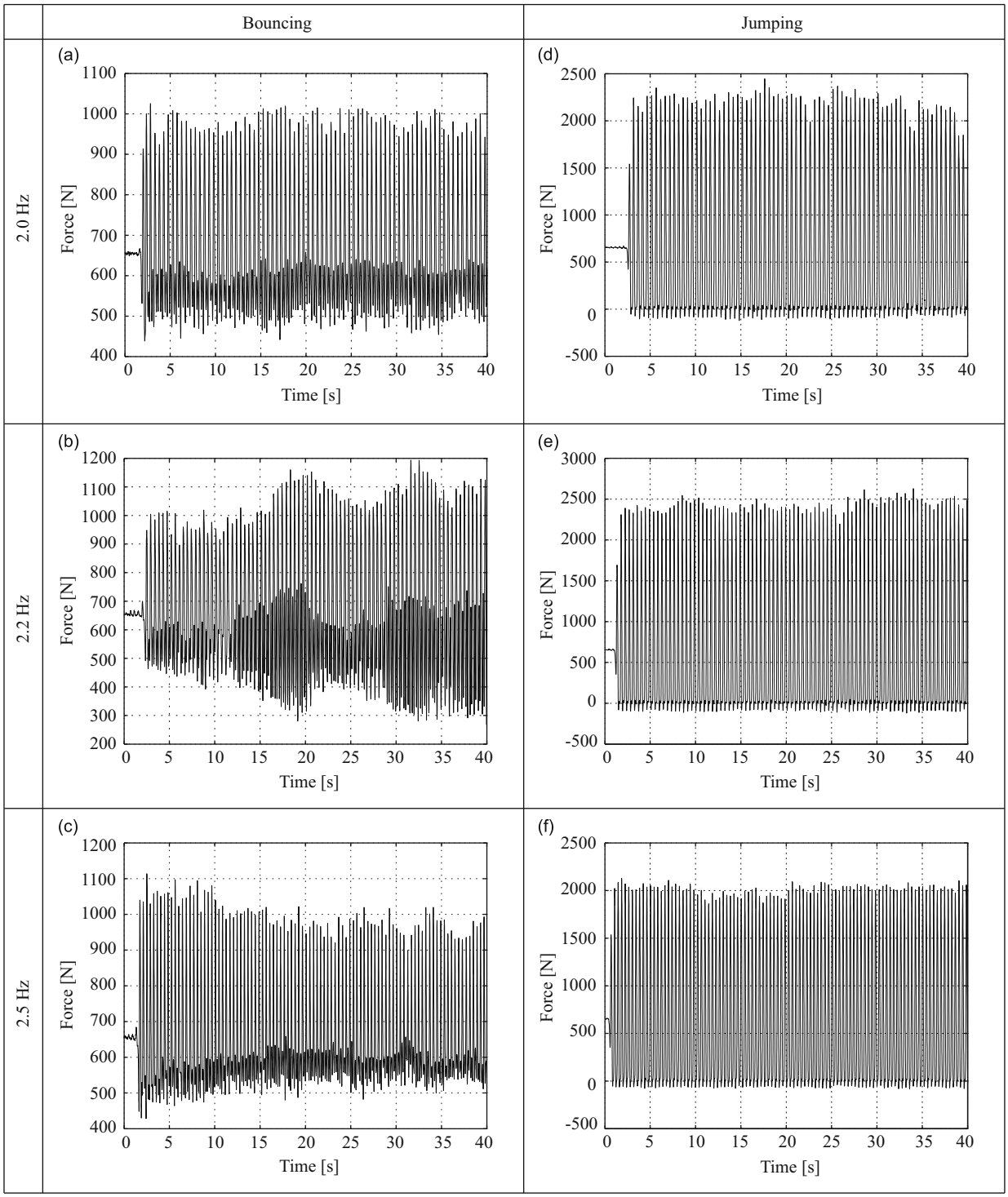

Fig. 12. Reproduced force time histories generated by TS 1 when (a–c) bouncing and (d–f) jumping on the test structure in response to regular metronome beats at 2, 2.2 and 2.5 Hz.

to follow the metronome beat when the structure was dynamically excited in resonance, i.e. they varied more their jumping/bouncing rate when structural responses were greater. As noted elsewhere [25], the most likely explanation for this happening is the influence of large levels of the resonant structural response on the ability of the test subjects to keep jumping/bouncing regularly. This is because the human body is a very sensitive vibration receiver characterised by the innate ability to adapt quickly to almost any type and level of vibration which normally occurs in nature [26].

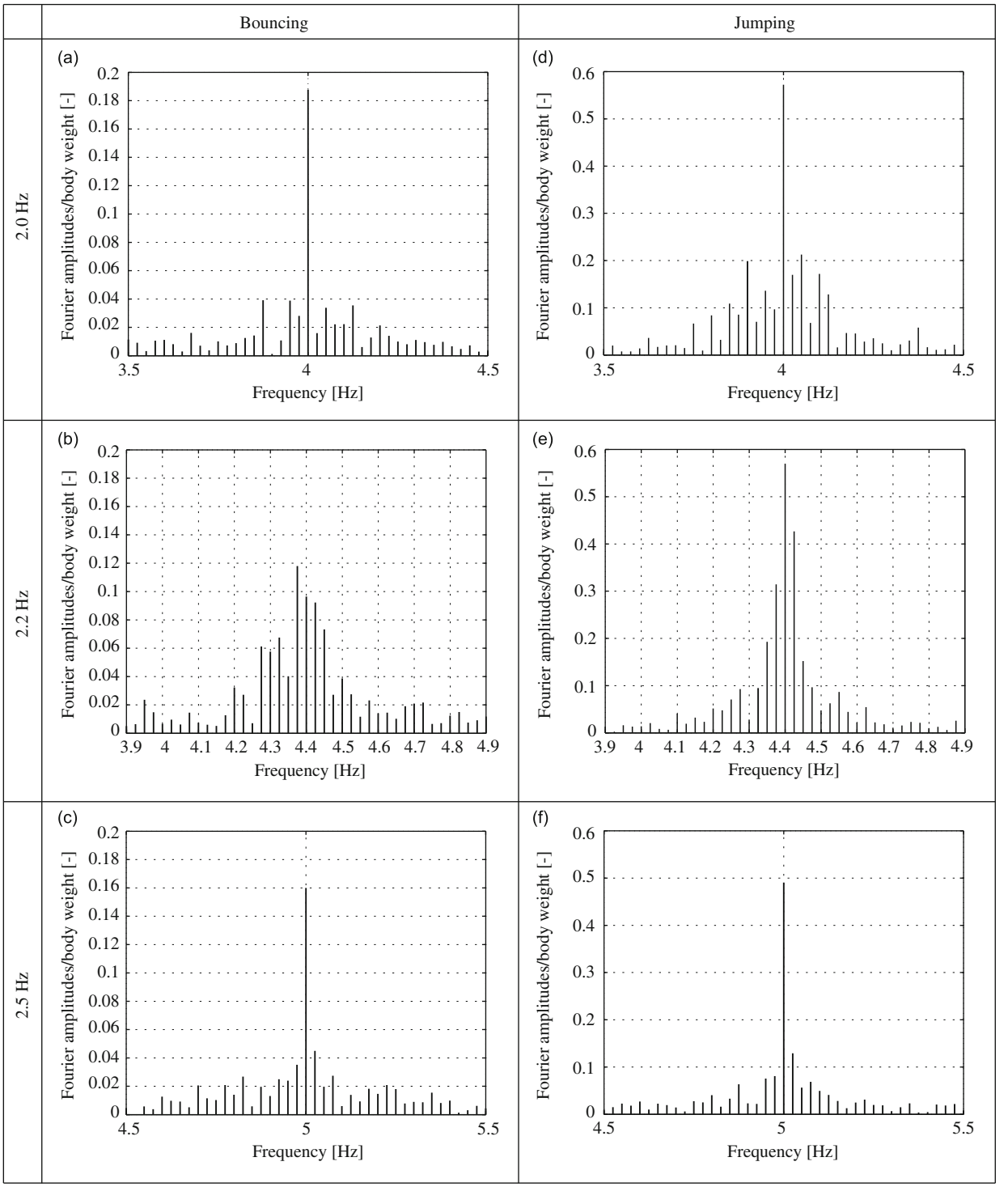

Fig. 13. Fourier amplitudes in the vicinity of the second dominant harmonic calculated using 40 s of the force signals illustrated in Fig. 12.

In qualitative feedback after the experiments, both test subjects agreed that non-resonant vibrations of the structure were barely perceptible, whereas the resonant response levels were perceived as rather excessive, sometimes even 'scary', thus influencing the way they were moving on the structure. Moreover, they reported that the effect was dominant for bouncing, where the feet are in permanent contact with the vibrating structure. This is also supported by comparison between the Fourier amplitude spectra of bouncing and jumping resonant forces given in Fig. 13b and e. Apparently, the spread of energy is more pronounced in the case of bouncing, illustrating greater disturbance in the regular bouncing rhythm.

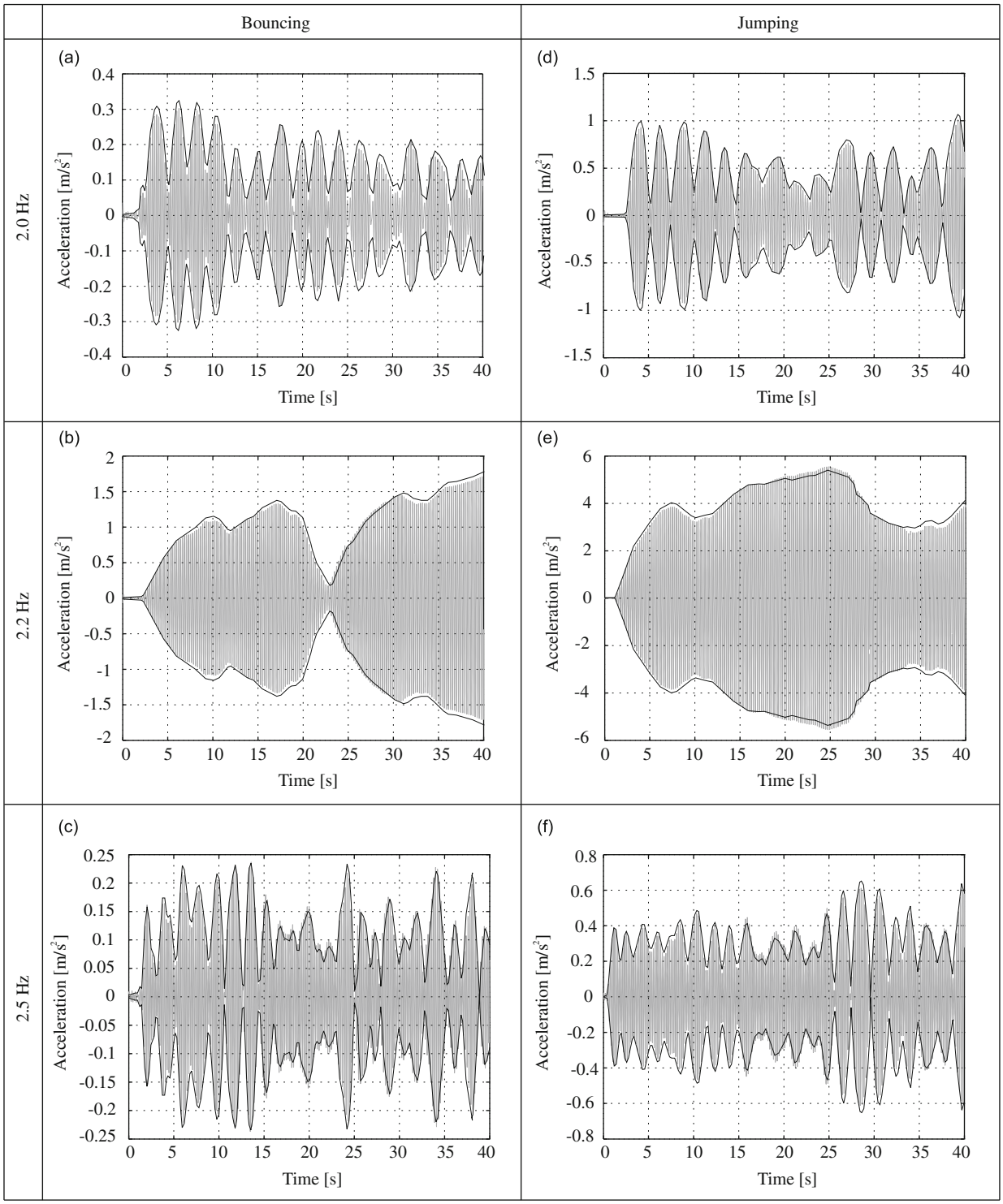

Fig. 14. Measured (grey) and envelope of simulated (black) accelerations of the structure due to TS 1 jumping/bouncing in the middle of the span.

4.2.2. Two test subjects

Following the same logic from the previous section, a nominally identical analysis was carried out based on the motion data recorded for both test subjects bouncing and jumping together at the mid-span of the structure in response to regular metronome beats at 2, 2.2 and 2.5 Hz (Section 3.4). The reproduced force time histories are given in Fig. 15.

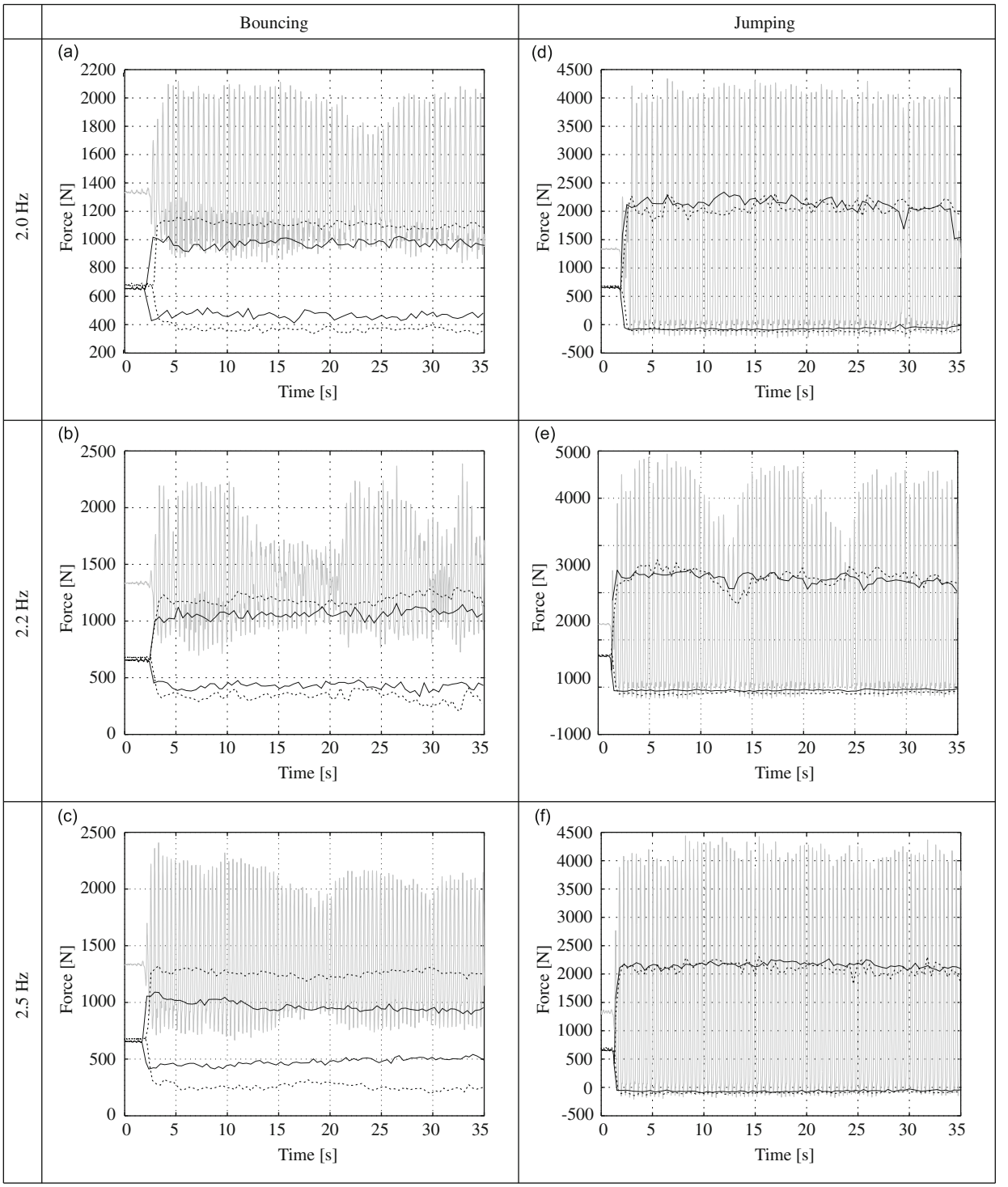

Fig. 15. Force time histories generated by TS 1 (black), TS 2 (dashed) and their sum (grey) when (a–c) bouncing and (d–f) jumping in response to regular metronome beats at 2, 2.2 and 2.5 Hz.

As a proof of successful force reproduction for all jumping/bouncing rates, Fig. 16 illustrates a good match between the measured vibration responses (Section 3.4) and those calculated from the corresponding SDOF model using the reproduced forces and the nonlinear modal properties.

Although the test subjects were following the same metronome beats when jumping and bouncing together, there was a sporadic lack of coordination between their movements, which is reflected in a lack of synchronisation of the

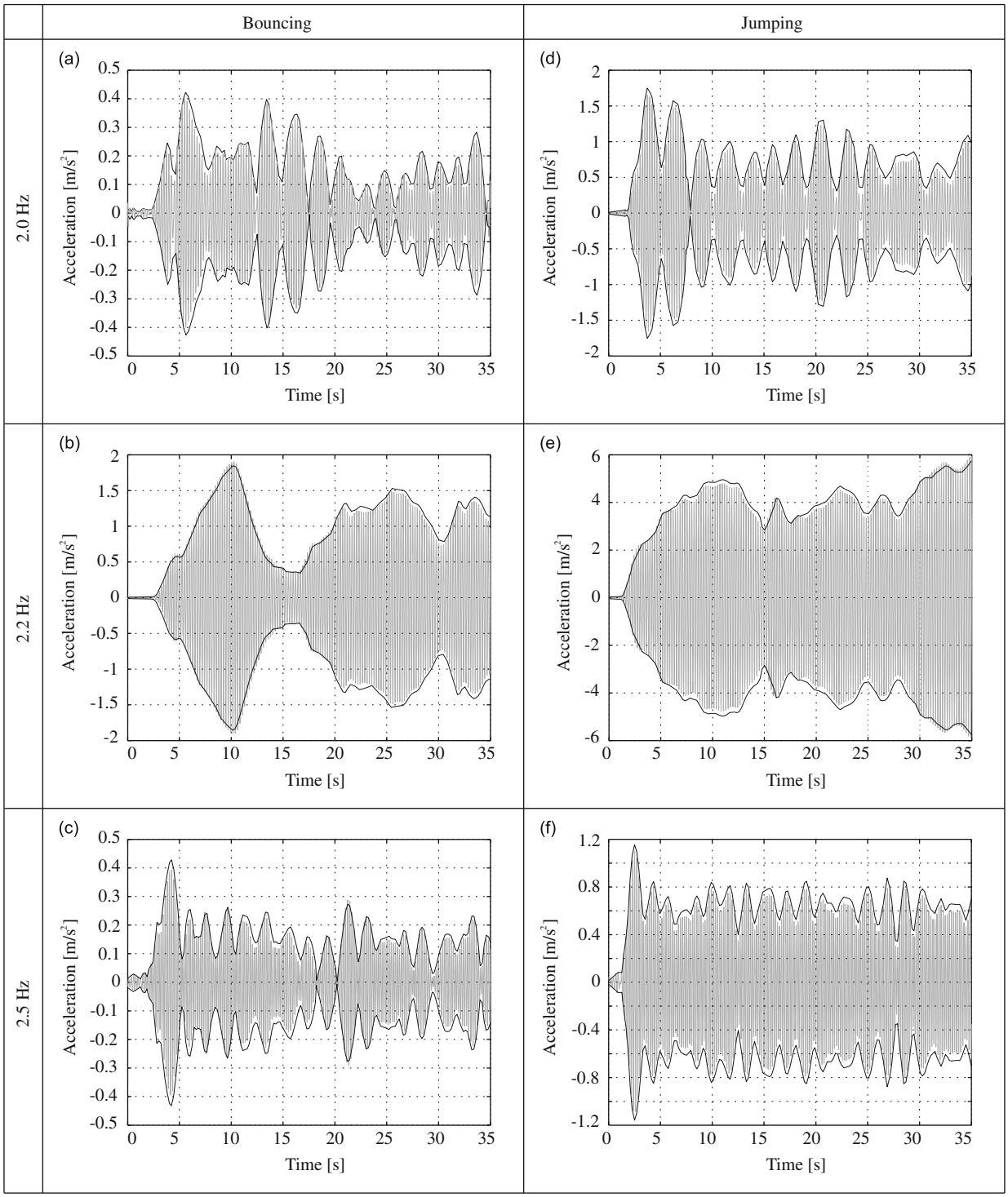

Fig. 16. Measured (grey) and envelope of simulated (black) mid-span vibration response of the structure due to two persons (a–c) bouncing and (d–f) jumping together at given regular metronome beats.

corresponding peak force amplitudes on a cycle-by-cycle basis (Fig. 17). Here, one jumping or bouncing cycle corresponds to a period needed to complete one jump or bounce.

In Fig. 17, there are cycles for which time instants of individual peak amplitudes match well, indicating a high synchronisation level. Also, this resulted in large peak amplitudes of the total sum force for these cycles. However, because

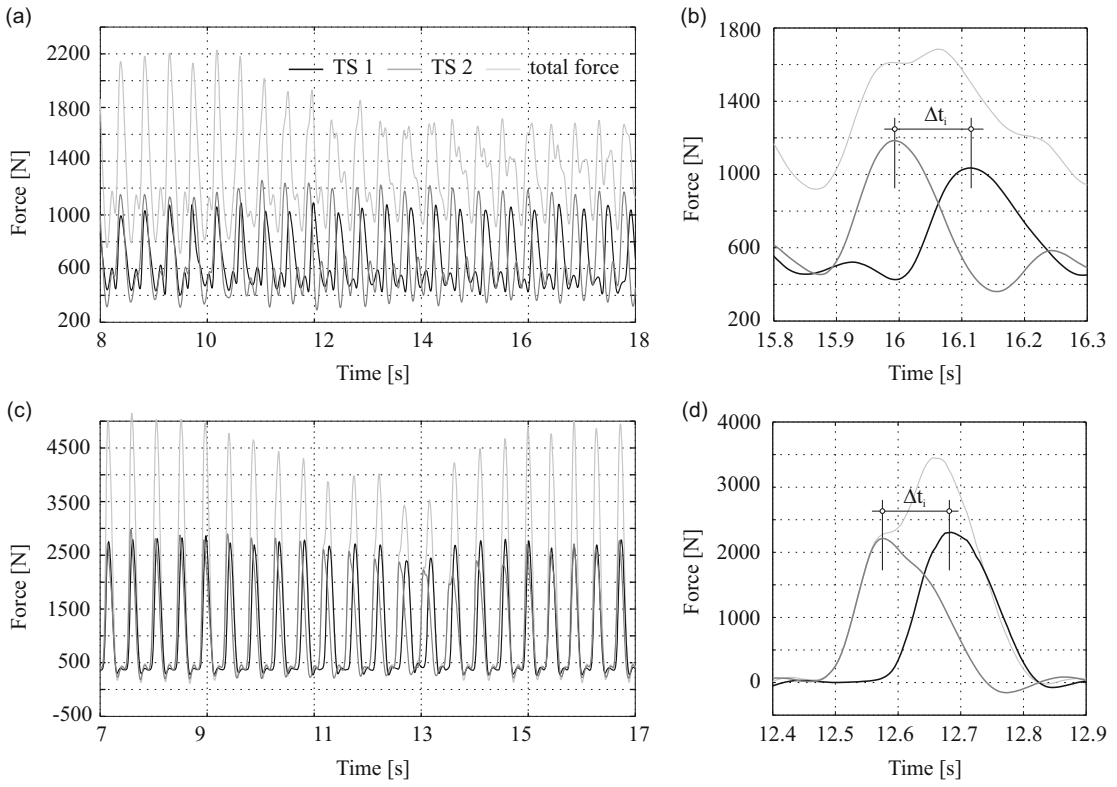

Fig. 17. Synchronisation of (a, b) bouncing and (c, d) jumping forces at 2.2 Hz. Figs. 15 and 17 illustrate the same data.

Table 1
Summary of statistics (mean ± standard deviation) of Δt_i parameters extracted from Fig. 15.

Frequency (Hz)	Bouncing (s)	Jumping (s)
2.0	0.052 ± 0.036	0.039 ± 0.020
2.2	0.076 ± 0.076	0.073 ± 0.036
2.5	0.049 ± 0.024	0.022 ± 0.012

humans are not machines, despite the metronome beat they could not keep moving in synchronisation for a long time, causing peaks to diverge and their sum to decrease. After a while, the process starts to reverse, i.e. the peaks start moving towards each other and finally meet, being synchronised again. Therefore, the lack of synchronisation can be quantified through relative changes of time lags Δt_i between peaks of individual force signals on a cycle-by-cycle basis (Fig. 17). A summary of mean values and standard deviations of Δt_i values extracted from 30 s duration signals (between 5 and 35 s out of a 35 s long test) in Fig. 17 is given in Table 1.

The largest values of the mean and standard deviation are for the excitation causing near-resonant response for both bouncing and jumping indicating that the synchronisation was most affected by the large structural vibrations. Also, for both resonant and non-resonant rates, synchronisation during jumping was better compared with the bouncing counterparts.

When comparing the vibration levels in Fig. 14 and their counterparts in Fig. 16, it can be noticed that the structural response due to human-induced dynamic forces is not a linear superposition of the individual responses. For example, two persons generated the same level of resonant response as the single TS jumping or bouncing alone. This suggests that individual contributions to vibrations are very often reduced for some reason when more than one person participates in the exercise. The next section deals with these issues by studying the energy flow in the joined human–structure system.

4.2.3. Energy flow and power

A useful technique for studying human–structure dynamic interaction involves analysis of the power developed by human occupants moving on a structure and the power represented by the rate of internal energy dissipation in a structure conceptualised via damping forces [27]. Energy, with the units of Joules (J) or (Nm), is the time integral of power and is a

more familiar quantity whose flow is easy to visualise. However graphical representation using power, with units of Watts (W) or (Nm/s), is simpler to study for comparative purposes.

For the slab strip, supply of energy to the structure at the point of contact is the instantaneous product of velocity $\dot{x}(t)$ and contact force $f(t)$. The contact force $f(t)$ could be obtained either directly by a load cell or by reproduction from the marker motion, while velocity could be obtained by integrating accelerometer signals or by differentiating contact point marker displacements. Here, the contact force is measured indirectly using Eq. (2) and the velocity is obtained from displacements of a marker attached to the middle of the span where the activity was happening.

Consider an equation of motion of a SDOF system, e.g. the first mode of vibration of the slab strip excited by a jumping force at the midpoint (antinode). If the mode shape is unity scaled at the midpoint then modal and physical displacements at the mid-point are identical and both can be represented by $x(t)$, which is a solution of the following well known differential equation [28]:

$$m\ddot{x}(t)+c(a)\dot{x}(t)+k(a)x(t)=f(t) \tag{7}$$

Multiplying by the modal/physical velocity $\dot{x}(t)$, the equation of motion can be used to calculate instantaneous power $f(t)\dot{x}(t)$:

$$m\ddot{x}(t)\dot{x}(t)+c(a)\dot{x}^2(t)+k(a)x(t)\dot{x}(t)=f(t)\dot{x}(t) \tag{8}$$

Here, $m\ddot{x}(t)\dot{x}(t)$ is kinetic power, $c(a)\dot{x}^2(t)$ is damping power and $k(a)x(t)\dot{x}(t)$ is potential power.

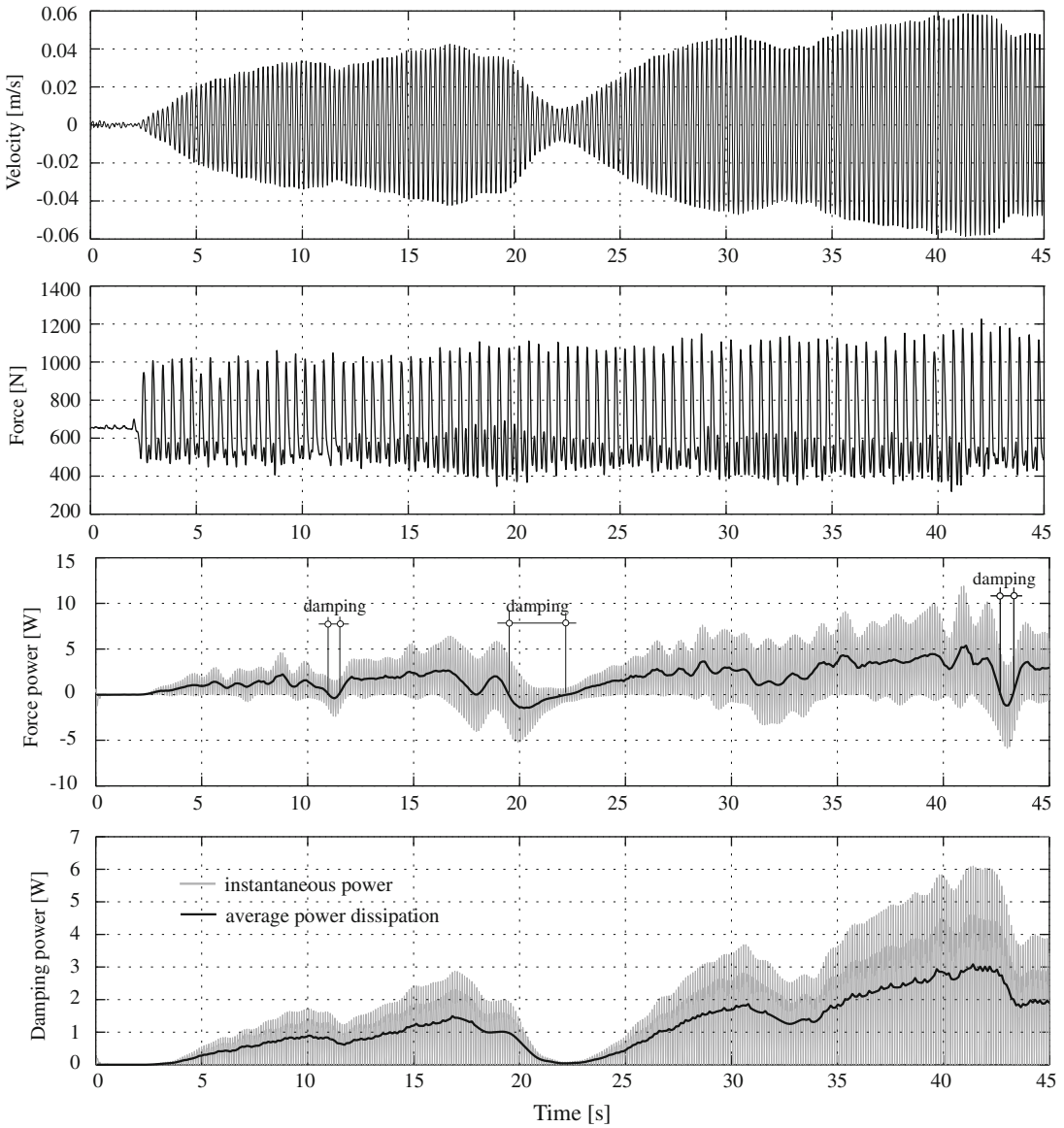

Fig. 18. Energy flow and power due to TS 1 bouncing in the middle of the span at resonant rate of 2.2 Hz.

In resonance it is well known that the inertia and stiffness forces are perfectly balanced with the interchange of kinetic and potential energy resulting in a constant value of energy and no net supply to either of them. Simultaneously, the external force simply provides positive power to compensate for the energy dissipated internally via damping (damping power):

$$\begin{aligned} m\ddot{x}(t)\dot{x}(t) &= k(a)x(t)\dot{x}(t) \\ c(a)\dot{x}^2(t) &= f(t)\dot{x}(t) > 0 \end{aligned} \tag{9}$$

Away from resonance in steady state the damping power is always positive (due to the square term in $c(a)\dot{x}^2(t)$) but the external power has a zero-mean oscillating component with supply and withdrawal of energy during a cycle due to the imbalance of inertia and stiffness forces. During build up of response towards resonance the external force only supplies and never withdraws energy to build up the constant level of total (i.e. kinetic plus potential) energy.

In the case of a single TS bouncing, Fig. 18 shows positive power as response levels build up, with corresponding increasing damping power. The bouncing human power cycles below zero, sometimes because the response is off-resonance, but also sometimes because the TS is actually out of synchronisation with the motion, resulting in net removal of energy. The cycle-by-cycle average power, represented by the heavy line, shows whether the human is active (driving)

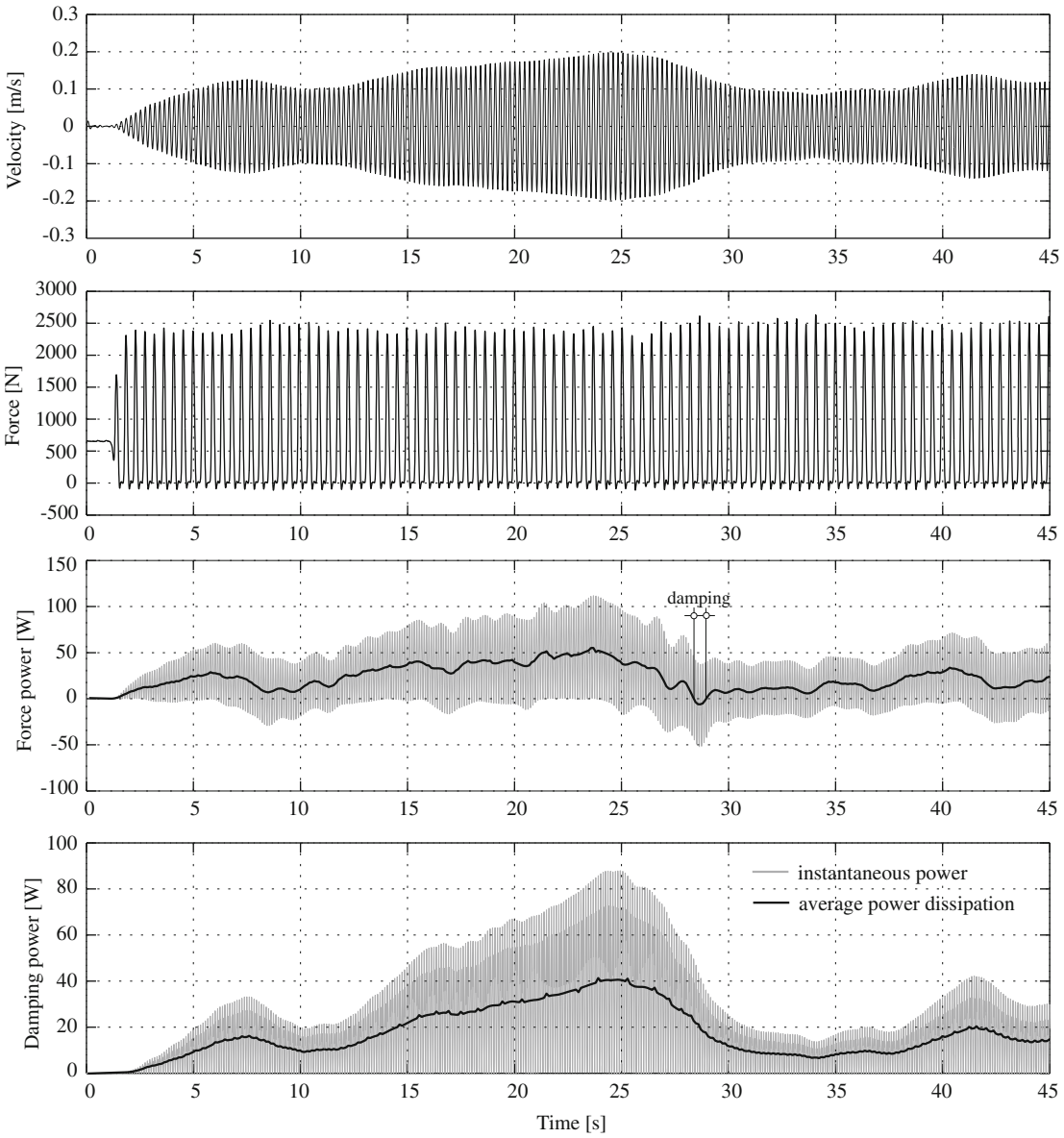

Fig. 19. Energy flow and power due to TS 1 jumping in the middle of the span at resonant rate of 2.2 Hz.

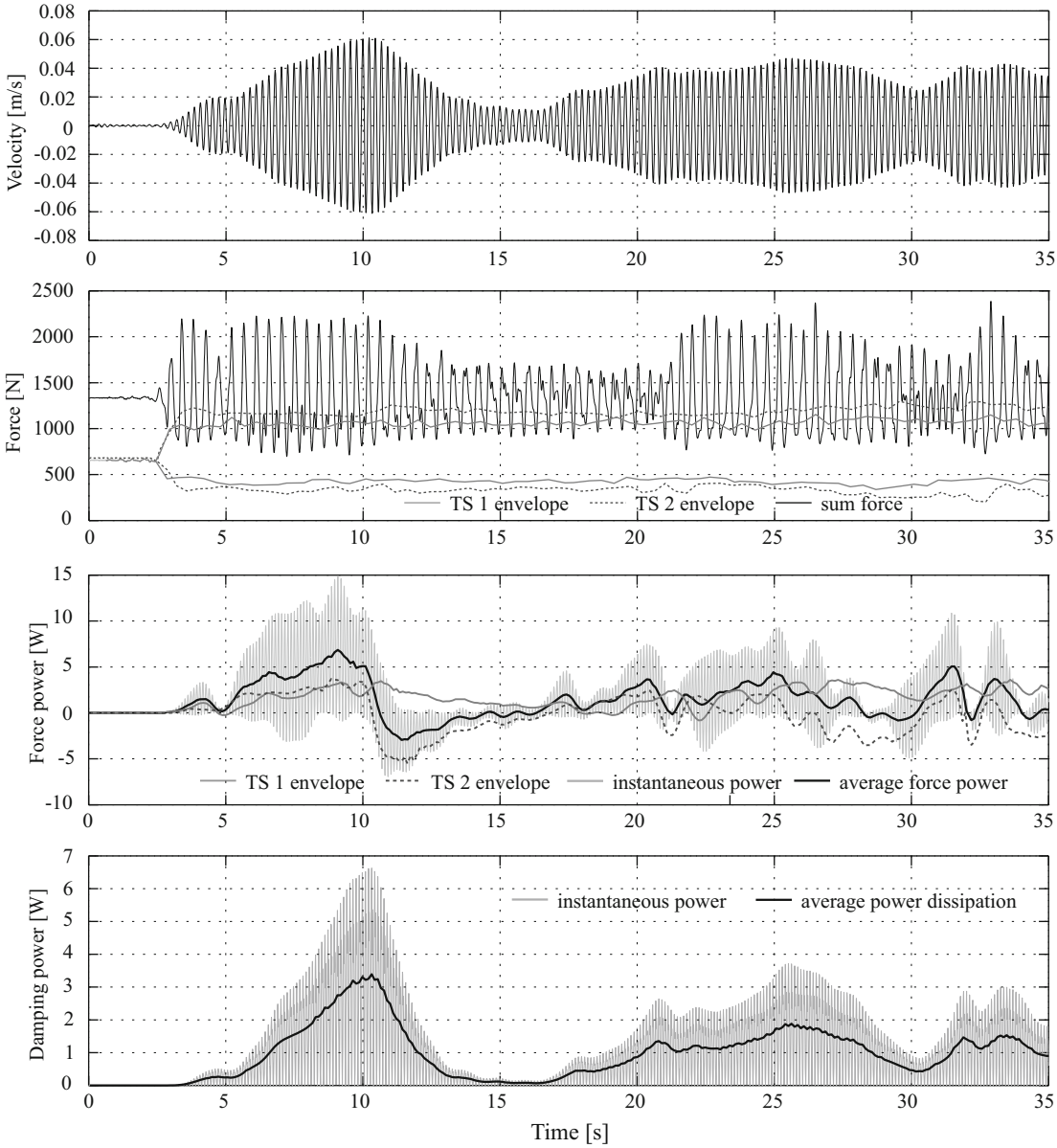

Fig. 20. Energy flow and power due to both TSs bouncing together in the middle of the span at resonant rate of 2.2 Hz.

or passive (damping) overall. Fig. 19 shows the same effect for jumping, but note that the power levels are an order of magnitude greater.

For the two TSs bouncing/jumping together (Figs. 20 and 21), the individual cycle-by-cycle average power plots show that TS 1 was supplying energy to the system most of the time during the tests, while TS 2 was often acting as the strong damping element. This clearly explains why the resonance was very difficult to maintain for both activities (Fig. 16). These tests also confirmed findings elsewhere [29] that the humans are characterised by huge inter-subject differences between their abilities to induce dynamic loads, to change the dynamic properties and to respond to nominally the same vibrations of the structure they occupy and dynamically excite.

5. Conclusions

This paper presents a novel method in the civil engineering context to measure indirectly bouncing and jumping GRFs by combining human body motion tracking data and known/assumed body mass distribution.

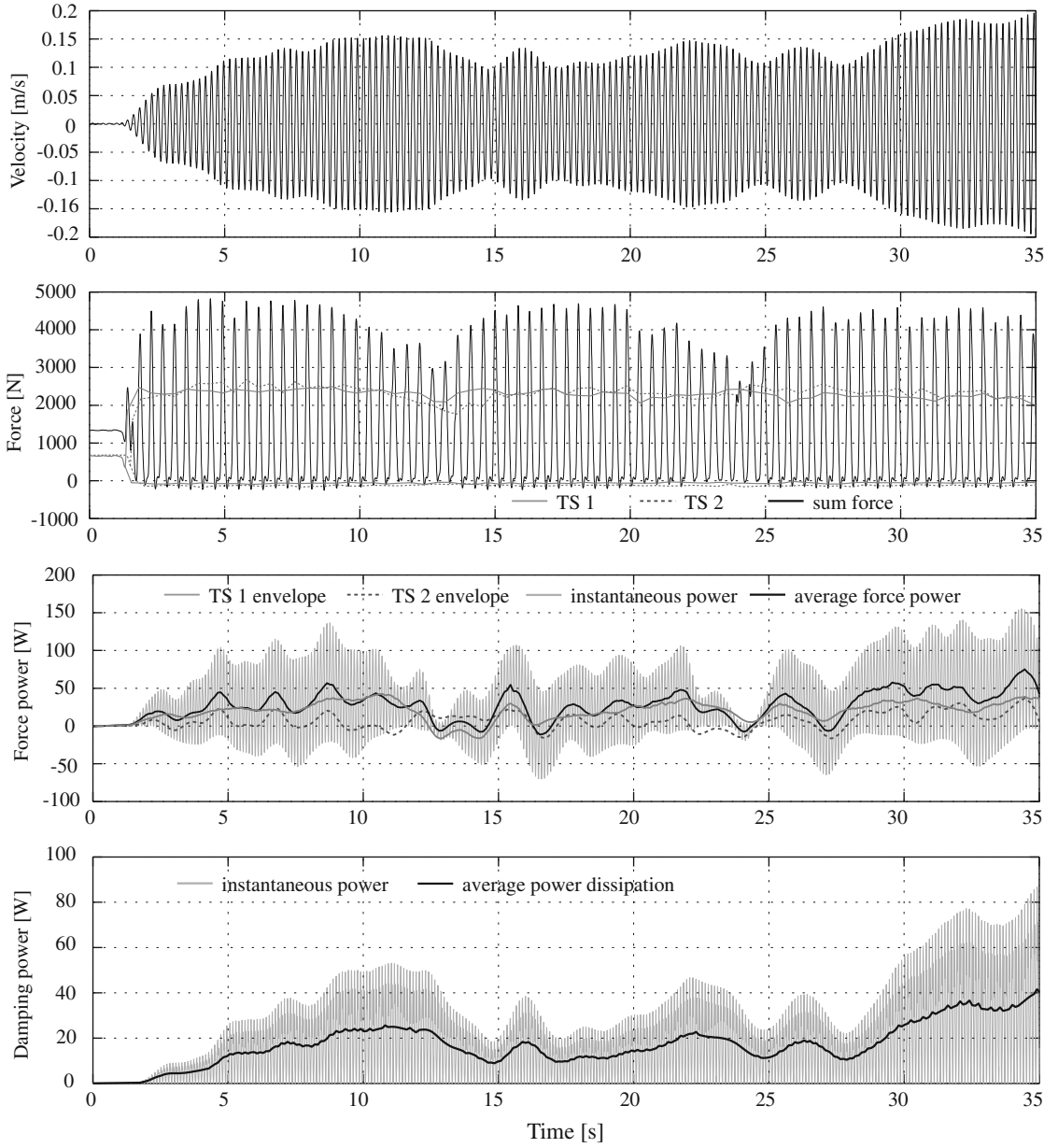

Fig. 21. Energy flow and power due to both TSs jumping together in the middle of the span at resonant rate of 2.2 Hz.

When compared with the traditional direct force measurements on floor-mounted force plates, a key advantage of the method proposed is utilisation of 'free-field' measurement of continuous bouncing and jumping GRFs. As demonstrated, indirect force measurements enable assessment of structures, such as grandstands and entertainment venues, predominantly occupied and dynamically excited by bouncing/jumping humans. Moreover, the method enables study of areas of significant interest and uncertainty, specifically human–structure dynamic interaction and synchronisation between occupants when bouncing and jumping on flexible structures. Measurements have been able to show the negative cue effect of perceptible vibrations on the GRFs. Also, they indicated that in the joint human–structure dynamic system an active human can, not only be the source of energy, but can also act as the strongest damping element. This happens either because the response is off-resonance or because of phase difference with the structural motion resulting in net removal of energy. The effect is even stronger for multiple occupants due to the lack of synchronisation of their movements.

The method piloted in this paper has been validated using two male participants, who were jumping or bouncing either individually or as a pair on a realistic test structure.

This means that there remains a requirement to carry out similar tests for single individuals and multiple occupants moving on a number of different, more or less vibrating real-life structures. Measurements can be used to develop and

calibrate a new generation of badly needed models of rhythmic crowd loads. Therefore, this approach presents a timely opportunity to advance the whole field of vibration serviceability assessment of structures predominantly occupied and dynamically excited by bouncing/jumping humans, such as grandstands and entertainment venues.

Acknowledgements

The authors would like to thank Mr. Christopher Middleton, Dr. Ivan Munoz-Diaz and Dr. Stana Zivanovic for their help in collecting the data. Also, the authors would like to acknowledge the financial support provided by the UK Engineering and Physical Sciences Research Council (EPSRC) for Grant reference EP/E018734/1 ('Human Walking and Running Forces: Novel Experimental Characterisation and Application in Civil Engineering Dynamics').

References

[1] R.C. Batista, C. Magluta, Spectator-induced vibration of Maracana Stadium, *Second European Conference on Structural Dynamics EURODYN*, Trondheim, Norway, June 1993.
[2] D. Rogers, Two more 'wobbly' stands, *Construction News*, 17 August 2000.
[3] D. Parker, Rock fans uncover town hall floor faults, *New Civil Engineer*, 20 November 2003.
[4] A. Ebrahimpour, R.L. Sack, W.E. Saul, G.L. Thinness, Measuring dynamic occupant loads by microcomputer, in: K.M. Will (Ed.), *Proceedings of the Ninth ASCE Conference on Electronic Computation,* New York, USA, 1986, pp. 328–338.
[5] G. Pernica, Dynamic load factors for pedestrian movements and rhythmic exercises, *Canadian Acoustics* 18 (2) (1990) 3–18.
[6] J.H. Rainer, G. Pernica, D.E. Allen, Dynamic loading and response of footbridges, *Canadian Journal of Civil Engineering* 15 (1) (1988) 66–71.
[7] D.A. Winter, *Biomechanics and Motor Control of Human Movement*, second ed., John Wiley & Sons, Toronto, Canada, 1990.
[8] J. Perry, *Gait Analysis: Normal and Pathological Function*, Thorofare, New York, USA, 1992.
[9] AMTI User Manuals, Advanced Mechanical Technology Inc., Watertown, MA, USA, 2008.
[10] A.B. Thorton-Trump, R. Daher, The prediction of reaction forces from gait data, *Journal of Biomechanics* 8 (1975) 173–178.
[11] D.I. Miller, M.A. Nissinen, Critical examination of ground reaction force in the running forward somersault, *International Journal of Sport Biomechanics* 3 (1987) 189–206.
[12] M.M. Bobbert, H.C. Schamhardt, B.M. Nigg, Calculation of vertical ground reaction force estimates during running from positional data, *Journal of Biomechanics* 24 (1991) 1095–1105.
[13] Sir I. Newton, in: E. Halley (Ed.), *Philosophiae Naturalis Principia Mathematica* (*Mathematical Principles of Natural Philosophy*), London, UK, 1687.
[14] W.T. Dempster, Space requirements of the seated operator. Geometrical, kinematic, and mechanical aspects of the body with special reference to the limbs, Project no. 7214, Aerospace Medical Research Laboratory, Wright–Petterson Air Force Base, Ohio, USA, 1955.
[15] C.E. Clauser, J.T. McConville, J.W. Young, Weight, volume and centre of mass of segments of the human body, Technical Report 69–70, Aerospace Medical Research Laboratory, Wright–Petterson Air Force Base, Ohio, USA, 1969.
[16] V. Zatsiorsky, V. Seluyanov, The mass and inertia characteristics of the main segments of the human body, in: H. Matsui, K. Kobayashi (Eds.), *Biomechanics VIII-B*, Human Kinetic, Illinois, USA, 1983, pp. 1152–1159.
[17] P. de Leva, Adjustments to Zatsiorsky–Seluyanov's segment inertia parameters, *Journal of Biomechanics* 29 (9) (1996) 1223–1230.
[18] A. Cappozzo, A. Leardini, U. Della Croce, L. Chiari, Human movement analysis using stereophotogrammetry. Part 1: theoretical background, *Gait Posture* 21 (2005) 186–196.
[19] V. Racic, A. Pavic, J.M.W. Brownjohn, Experimental identification and analytical modelling of human walking forces: literature review, *Journal of Sound and Vibration* 326 (2009) 1–49.
[20] Codamotion User Manuals, Charnwood Dynamics Ltd., Leicestershire, UK, 2009.
[21] D. Ginty, J.M. Dervent, T. Ji, The frequency ranges of dance-type loads, *The Structural Engineer* 79 (6) (2001) 27–31.
[22] APS-113 User Manual, Acoustic Power Inc., Carlsbad, USA, 2009.
[23] QA750 User Manual, Honeywell International Inc., Washington, USA, 2009.
[24] J.M.W. Brownjohn, H. Hao, T.-C. Pan, Assessment of structural condition of bridges by dynamic measurements, Applied Research Project RG5/97, NTU School of CSE, Singapore, April 2001.
[25] S. Yao, J.R. Wright, A. Pavic, P. Reynolds, Experimental study of human-induced dynamic forces due to jumping on a perceptibly moving structure, *Journal of Sound and Vibration* 296 (2006) 150–165.
[26] M.J. Griffin, *Handbook of Human Vibration*, Academic Press, London, UK, 1996.
[27] J.M.W. Brownjohn, Energy dissipation from vibrating floor slabs due to human–structure interaction, *Shock and Vibration* 8 (2001) 315–323.
[28] R.W. Clough, J. Penzien, *Dynamics of Structures*, McGraw-Hill Inc., Singapore, 1993.
[29] H. Bachmann, A.J. Pretlove, H. Rainer, Dynamic forces from rhythmical human body motions, Appendix G, in: *Vibration Problems in Structures: Practical Guidelines*, Birkhäuser Verlag, Basel, Switzerland, 1995.